

# Antibacterial Activity of Membrane-Permeabilizing Bactericidal Cyclodextrin Derivatives

Hatsuo Yamamura,\* Tatsuya Hagiwara, Yuma Hayashi, Kayo Osawa, Hisato Kato, Takashi Katsu, Kazufumi Masuda, Ayumi Sumino, Hayato Yamashita, Ryo Jinno, Masayuki Abe, and Atsushi Miyagawa



Cite This: *ACS Omega* 2021, 6, 31831–31842



Read Online

ACCESS |



Metrics & More

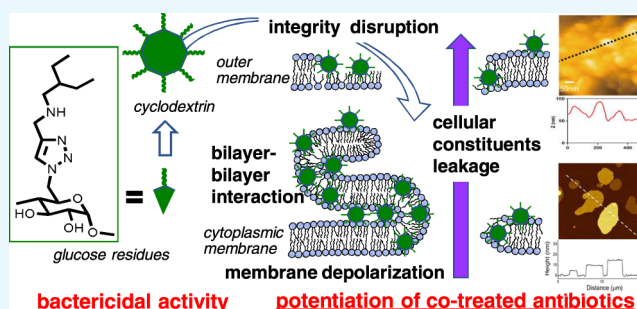


Article Recommendations



Supporting Information

**ABSTRACT:** Antimicrobial peptides that act by disrupting bacterial membranes are attractive agents for treating drug-resistant bacteria. This study investigates a membrane-disrupting peptide mimic made of a cyclic oligosaccharide cyclodextrin scaffold that can be chemically polyfunctionalized. An antibacterial functional group on the peptide was simplified to an alkylamino group that combines cationic and hydrophobic moieties, the former to interact with the anionic bacterial membrane and the latter with the membrane interior. The cyclodextrins equipped with eight alkylamino groups on the molecules using a poly-click reaction exhibited antibacterial activity against Gram-positive and Gram-negative bacteria, including drug-resistant pathogens such as carbapenem-resistant *Enterobacteriaceae*. Several lines of evidence showed that these agents disrupt bacterial membranes, leading to rapid bacterial cell death. The resulting membrane perturbation was directly visualized using high-speed atomic force microscopy imaging. In Gram-negative bacteria, the membrane-permeabilizing action of these derivatives allowed the entry of co-treated traditional antibiotics, which were then active against these bacteria.



## INTRODUCTION

The increasing number of multidrug-resistant strains of bacteria has created an urgent need for new types of antibiotics.<sup>1</sup> Antimicrobial peptides are attractive candidates<sup>2–5</sup> because their mechanism of action differs from that of traditional antibiotics. These peptides attack the bacterial membrane directly rather than affecting a metabolic pathway. Positively charged amino groups in the peptides interact with the negatively charged surface of the bacterial cell membrane, and their hydrophobic groups interact with nonpolar lipid acyl chains in the membrane. These interactions lead to the disruption of the bacterial cell membrane. Antimicrobial peptides exhibit strong bactericidal activity and broad-spectrum antibacterial activity.<sup>6,7</sup> However, the high structural complexity of the peptides makes their synthesis difficult and costly, hampering efforts to improve their antibacterial activity and decrease their toxicity to animal cells. As a result, only a limited number of peptides are now in clinical use.

Our previous studies investigated the antimicrobial peptide gramicidin S and its chemical derivatives.<sup>8–10</sup> This large  $\beta$ -sheet-forming cyclic decapeptide (diameter, 1 nm) has two amino groups that interact with the anionic bacterial cell surface and hydrophobic alkyl and aryl groups that interact with the inner hydrophobic components of the bacterial cell membrane. The peptide exhibits strong antibacterial activity against Gram-positive bacteria but only weak activity against Gram-negative bacteria. In contrast, the antimicrobial cyclic

peptide polymyxin B, which has five cationic residues and a fatty acid tail, exhibits strong activity against Gram-negative bacteria.<sup>11</sup> Consistent with this observation, we found that the addition of amino and hydrophobic groups to the gramicidin S molecule resulted in a derivative that exhibited good antimicrobial activity against both Gram-positive and Gram-negative bacteria.<sup>10</sup> Thus, the number and ratio of cationic and hydrophobic groups appear to affect the antibacterial activity strength and selectivity. These results prompted us to ask whether the presence of a suitable number of each type of functional group (amino and hydrophobic groups) can confer antibiotic activity to a molecule, even one with a nonpeptide base. This study aims to answer this question by investigating the antibacterial activity of derivatives of cyclodextrin, a cyclic oligosaccharide composed of D-glucose residues. Cyclodextrin was chosen as the molecular scaffold because its diameter of 1 nm matches that of antimicrobial cyclic peptides, and it can be chemically polyfunctionalized using a modification method previously employed in studies of molecular recognition.<sup>12,13</sup> In this study, we present chemically modified  $\gamma$ -cyclodextrin

Received: August 20, 2021

Accepted: October 29, 2021

Published: November 15, 2021



ACS Publications

© 2021 The Authors. Published by  
American Chemical Society

31831

<https://doi.org/10.1021/acsomega.1c04541>  
*ACS Omega* 2021, 6, 31831–31842

Scheme 1. Syntheses of Cyclodextrins 1–15

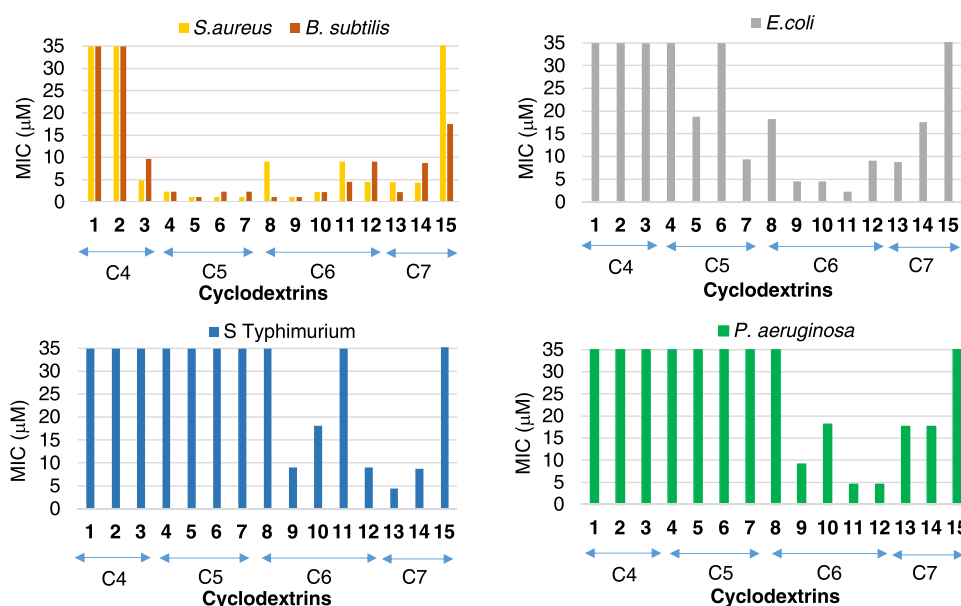
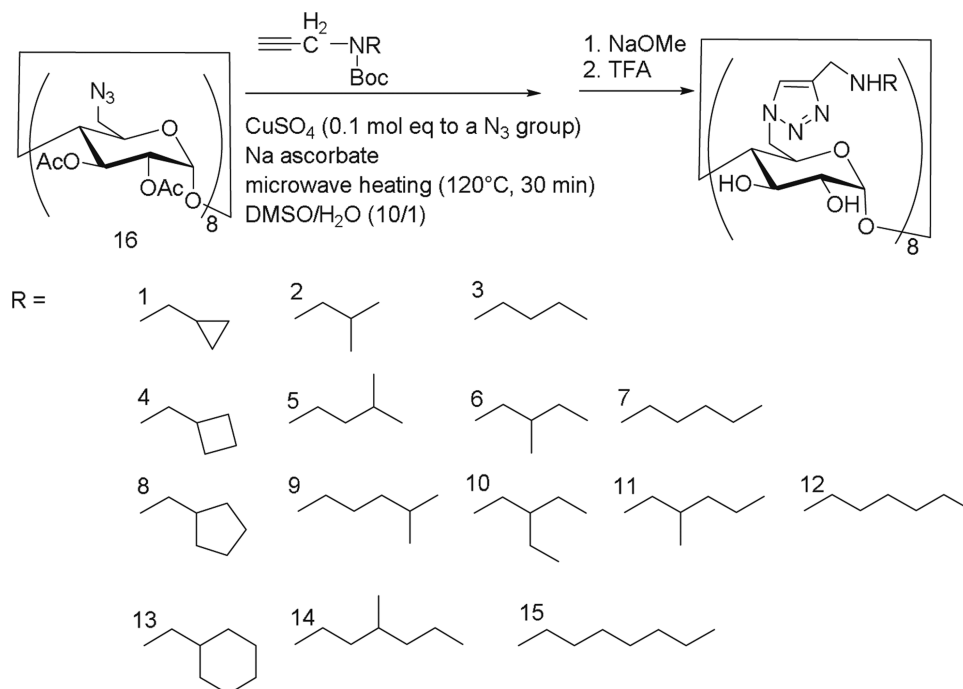


Figure 1. Minimum inhibitory concentrations (MICs) of alkylamino cyclodextrin derivatives 1–15 against drug-sensitive bacteria.

derivatives against not only Gram-positive but also Gram-negative bacteria, including drug-resistant pathogens.

## RESULTS AND DISCUSSION

**Chemical Modification of Cyclodextrin.** Antimicrobial peptides have poly-cationic amino groups such as lysine and ornithine and poly-hydrophobic alkyl groups such as 1-methylethyl groups of valine and 2-methylpropyl groups of leucine. Using a cyclodextrin scaffold, we were able to simplify the peptide structure as follows: (1) a hydrophobic moiety and a cationic moiety were combined into an alkylamino group and (2) only one type of alkylamino group was attached to each of the glucose residues in a cyclodextrin molecule such that each

$\gamma$ -cyclodextrin derivative has eight of the same alkylamino-modified glucoses.<sup>14</sup> For versatile poly-alkylamino functionalization of a cyclodextrin molecule, we adopted a microwave (MW)-assisted Huisgen 1,3-dipolar cycloaddition method that was developed for the poly-modification of cyclodextrins.<sup>15–19</sup> Fifteen types of  $\gamma$ -cyclodextrin derivatives 1–15 were prepared as reported previously,<sup>16,17</sup> adding linear, branched, and cyclic alkyl groups to their amino N atoms. A reaction of per-2,3-O-acetylated  $\gamma$ -cyclodextrin octaazide **16** with the corresponding *tert*-butoxycarbonyl (Boc)-protected propargyl-alkylamines via the MW-assisted click reaction and subsequent deprotection attached eight of each alkylamino group to a  $\gamma$ -cyclodextrin molecule (Scheme 1). The click reaction for introducing eight alkylamino functional groups was completed in 30 min by MW

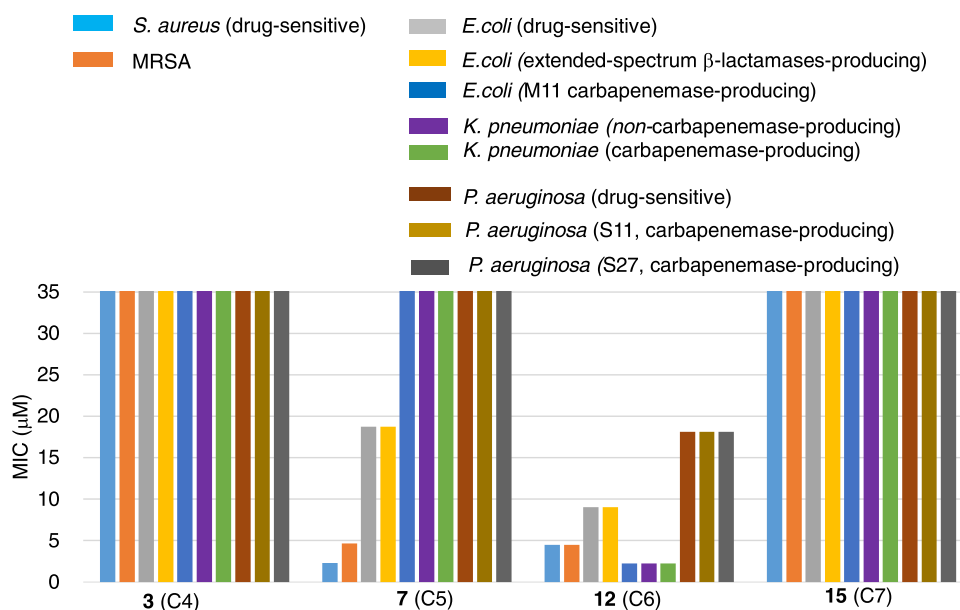


**Figure 2.** Minimum inhibitory concentrations (MICs) of *n*-alkylamino-modified cyclodextrins 3, 7, 12, and 15 against clinically isolated drug-resistant pathogens. *n*-Alkyl groups on N atoms of 3, 7, 12, and 15 were butyl, pentyl, hexyl, and heptyl groups, respectively.

heating (120 °C). Deprotection of the acetyl and Boc groups produced the desired cyclodextrins 1–15 as trifluoroacetic acid (TFA) salts for which the three-step overall yields were  $\approx 80\%$  or more. The success of the syntheses confirmed the advantage of using the MW-assisted click reaction method for molecular polyfunctionalization.

#### Antibacterial Activity of the Cyclodextrin Derivatives.

The antibacterial activity of the alkylamino-modified cyclodextrins against drug-sensitive bacteria was assessed. The minimum inhibitory concentrations (MICs) of the cyclodextrin derivatives against Gram-positive *Staphylococcus aureus* and *Bacillus subtilis* and Gram-negative *Escherichia coli*, *Salmonella* Typhimurium, and *Pseudomonas aeruginosa* are shown in Figure 1 and Table S1.<sup>20</sup> The antibacterial activity of the derivatives depended on the alkyl groups. Roughly speaking, the antibacterial activities of amino cyclodextrins bearing alkyl groups consisting of four carbon atoms (C4) 1–3 were weak. The amino cyclodextrins bearing alkyl groups consisting of five carbon atoms (C5) 4–7 and six carbon atoms (C6) 8–12 exhibited high antibacterial activity (MIC < 10  $\mu\text{M}$ ) against the Gram-positive *S. aureus* and *B. subtilis*. In the case of Gram-negative bacteria, all C6-alkyl derivatives exhibited high antibacterial activity against *E. coli*. The antibacterial activity of the cyclodextrins was comparable to that of melittin,<sup>21</sup> an antimicrobial peptide (MIC *S. aureus* 1–11  $\mu\text{M}$ , *E. coli* 3–22  $\mu\text{M}$ ). However, high antibacterial activity was observed against *S. Typhimurium* for only four of the C6 and C7-alkyl cyclodextrins (4-methylpentyl 9, *n*-hexyl 12, cyclohexylmethyl 13, and 3-methylhexyl 14) and against *P. aeruginosa* for only three C6-alkyl cyclodextrins (4-methylpentyl 9, 2-methylpentyl 11, and *n*-hexyl 12). Roughly speaking, little difference in antibacterial activity was observed between cyclic, linear, and branched alkyl structures if the number of carbon atoms was the same although antimicrobial peptides often contain amino acids with branched alkyl side chains of Val and Leu, and those who did not fit in this, such as 13–15, were also found.

Based on these results, we investigated the antibacterial activity of the linear *n*-alkyl-modified amino cyclodextrins 3, 7,

12, and 15 against the following clinically isolated drug-resistant pathogens: Gram-positive methicillin-resistant *S. aureus* (MRSA) and Gram-negative extended-spectrum  $\beta$ -lactamase-producing *E. coli*, carbapenemase-producing *E. coli*, *Klebsiella pneumoniae*, and *P. aeruginosa* (Figure 2; Table S2). The shortest *n*-butylamino cyclodextrin 3 (C4) exerted no antibacterial activity against any of the bacteria investigated here (MIC  $\geq 39 \mu\text{M}$ ). *n*-Pentylamino 7 (C5) was active against MRSA (MIC, 5  $\mu\text{M}$ ) but less active against the Gram-negative bacteria (MIC, 19–38  $\mu\text{M}$ ). In contrast, *n*-hexyl-modified amino 12 (C6) was antibacterial both against Gram-positive and Gram-negative bacteria. Although the MIC of this derivative against *P. aeruginosa* indicated moderate activity (18  $\mu\text{M}$ ), notably, the MIC against each of the carbapenem-resistant pathogens, *E. coli* and *K. pneumoniae*, was 2  $\mu\text{M}$ . All *n*-heptylamino 15 (C7) MICs were  $\geq 35 \mu\text{M}$ , and 15 exhibited much less antibacterial activity than did 3 (C4). The unique antibacterial activity exhibited by the C-5 and C6-alkyl-modified amino derivatives suggests that the carbon number of the alkyl moiety to which the amino group is attached affects the level of antibacterial activity. The MIC of each cyclodextrin against drug-resistant and drug-sensitive strains were quite similar, suggesting that the resistance mechanism is ineffective on these cyclodextrin derivatives. Previous studies<sup>17</sup> have shown that C5- and C6-alkylamino cyclodextrins are active against other Gram-positive drug-resistant bacteria, including *Streptococcus agalactiae* and *Enterococcus faecium*. Thus, the alkylamino cyclodextrin derivatives are likely promising for treating drug-resistant pathogens.

**Bacterial Cytoplasmic Membrane Disruption by Cyclodextrin Derivatives as Assessed by  $\text{K}^+$  Efflux.** The mechanism underlying the antibacterial activity of the cyclodextrin derivatives was investigated. First, we observed that the bacterial cytoplasmic membrane was disrupted by the cyclodextrins, as evidenced by inner  $\text{K}^+$  ion leakage from the bacterial cell. Bacteria contain large concentrations of  $\text{K}^+$  ion (100–500 mM) within their cells, and permeabilization of their cytoplasmic membranes causes ion efflux.<sup>22</sup> The  $\text{K}^+$  efflux from the bacterial cells caused by the treatment with *n*-

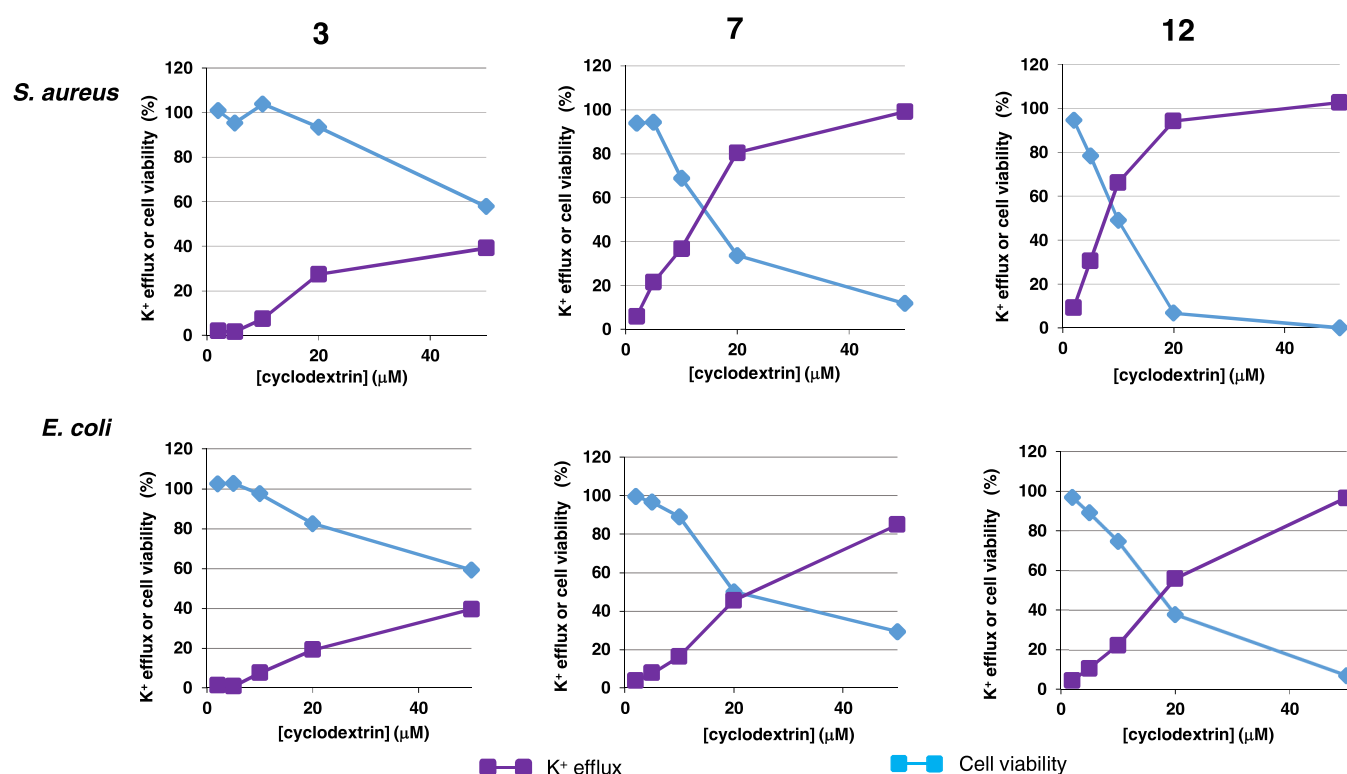


**Figure 3.** Dose-dependent K<sup>+</sup> efflux from *S. aureus* and cell viability upon treatment with alkylamino cyclodextrins 3, 7, and 12. *n*-Alkyl groups on N atoms of 3, 7, and 12 were butyl, pentyl, and hexyl groups, respectively. Purple line: K<sup>+</sup> efflux; blue line: cell viability.

alkylamino cyclodextrins 3, 7, and 12 was measured using a K<sup>+</sup> electrode (Figure 3).<sup>16</sup> The degree of K<sup>+</sup> efflux from Gram-positive *S. aureus* depended on the dose of the cyclodextrin derivative. The largest K<sup>+</sup> efflux was induced by *n*-hexylamino cyclodextrin 12 (94% at 20 μM), followed by pentylamino cyclodextrin 7 (80%). Butylamino cyclodextrin 3 induced the smallest K<sup>+</sup> efflux (38% at 20 μM). The observed degree of leakage correlated the observed antibacterial activity against *S. aureus* (Figure 1; Table S1). In addition, we observed that cell viability was inversely proportional to the K<sup>+</sup> efflux. Hexylamino cyclodextrin 12 (20 μM) caused 94% leakage of the cell contents and killed nearly all of the bacteria in 30 min. In the case of Gram-negative *E. coli*, hexylamino cyclodextrin 12 induced 56% K<sup>+</sup> efflux at 20 μM and 97% efflux at 50 μM, the largest efflux of the cyclodextrins examined here. As with *S. aureus*, the cell viability was inversely proportional to the dose. For all of the cyclodextrin derivatives tested, the K<sup>+</sup> efflux from *E. coli* was slightly lower than that from *S. aureus*, which correlates with the observed difference in antibacterial activity (MIC *E. coli* > MIC *S. aureus*). This difference may result from the outer membrane of Gram-negative *E. coli* acting as a barrier to permeation of the antibiotic molecules. Together, these results demonstrate that in Gram-positive bacteria, the cyclodextrin derivatives pass through the meshlike layer of peptidoglycan, reaching and disrupting the cytoplasmic membrane; in Gram-negative bacteria, these derivatives go through the outer membrane Gram-negative to reach and disrupt the inner cytoplasmic membrane.

**Bacterial Cytoplasmic Membrane Disruption by Cyclodextrin Derivatives as Assessed by Fluorescence Assay of Membrane Potential.** Membrane depolarization in *S. aureus* treated with the cyclodextrin derivatives was assessed using a membrane-potential-sensitive fluorescent probe

(DiSC<sub>3</sub>5). In control cells with fully intact cytoplasmic membranes, the fluorescent signal of the probe is quenched. Permeabilization of the membrane dissipates the membrane potential, which releases the probe into the medium, causing an increase in fluorescence.<sup>23</sup> Figure 4 shows the level of depolarization induced by each of the cyclodextrin derivatives as the fluorescence intensity relative to that of the membrane-pore-forming antimicrobial peptide melittin (1 μM).<sup>21</sup> Treatment of *S. aureus* with *n*-hexylamino cyclodextrin 12 (1 μM, corresponding to 20% MIC) caused a rapid increase in

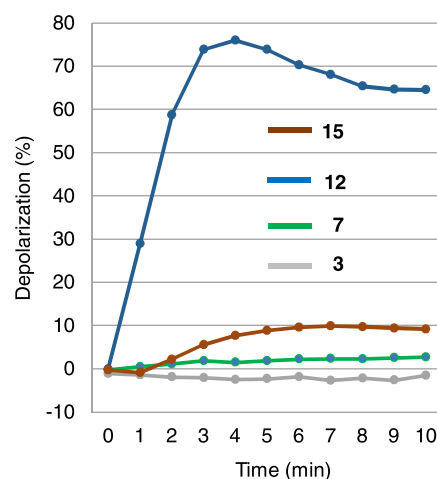


**Figure 4.** Depolarization of the cytoplasmic membrane potential of *S. aureus* as assessed by cyclodextrin (3, 7, 12, and 15, 1 μM)-induced changes in the fluorescence intensity of the membrane potential-sensitive dye DiSC<sub>3</sub>5. Depolarization is shown as the percent of that induced by 1 μM melittin.



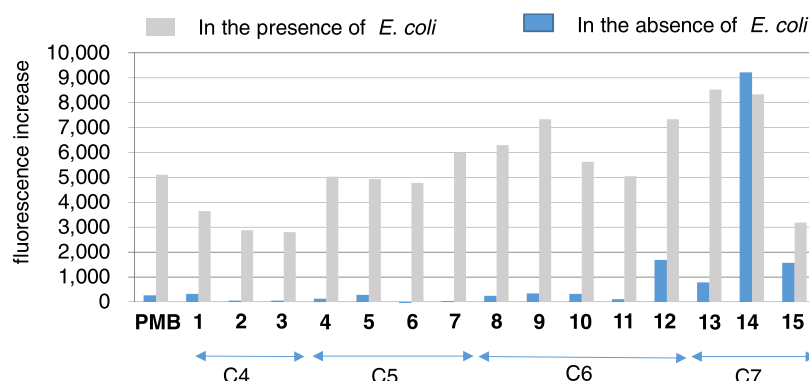


**Figure 5.** Influence of alkylamino cyclodextrins on the uptake of NPN by *E. coli* cells. Concentrations of butyl (1–4), pentyl (5–7), hexyl (8–12), and heptyl (13–15) amino cyclodextrins were 20, 19, 18, and 18  $\mu\text{M}$ , respectively, and that of polymyxin B (PMB) was 49  $\mu\text{M}$ .

fluorescence, reaching 75% of that induced by melittin in 3 min. This result shows that *n*-hexylamino cyclodextrin 12 rapidly disrupts the integrity of bacterial membranes, causing depolarization. Minimal membrane depolarization was observed for *n*-pentylamino cyclodextrin 7 (1  $\mu\text{M}$ ) because the dose was 9% of the MIC. In contrast, treatment with 10  $\mu\text{M}$  (89% of MIC) *n*-pentylamino cyclodextrin 7 caused 40% depolarization (data not shown). The observed proportionality of  $\text{K}^+$  leakage to cell death and membrane depolarization upon treatment with the alkylamino cyclodextrins strongly suggests that the mechanism underlying their antibacterial activity involves disruption of the cytoplasmic membrane.

#### Outer Membrane Disruption in Gram-Negative Bacteria as Assessed by Fluorescent Probe Uptake.

Perturbation of the Gram-negative bacterial outer membrane by the cyclodextrins was assessed by fluorescent probe uptake into the membrane. *N*-Phenyl-1-naphthylamine (NPN) is a hydrophobic fluorescent probe that emits a very weak fluorescence signal in an aqueous environment. Upon entry into a hydrophobic environment, such as a damaged membrane, the NPN fluorescence increases significantly.<sup>24</sup> Figure 5 shows the change in fluorescence induced by treatment with cyclodextrins possessing alkylamino groups. The hexyl (C6) amino derivatives 8–12 ( $\approx 20$   $\mu\text{M}$ ) caused a large increase in NPN fluorescence, comparable to that induced by the antimicrobial peptide polymyxin B (ca. 50  $\mu\text{M}$ ), a known disruptor of the outer membrane.<sup>25</sup> Together with the observed antibacterial activity and evidence of cytoplasmic membrane disruption, these results suggest that these cyclodextrin derivatives disrupt the outer membrane, enter the cytoplasm, and destroy the cytoplasmic membrane, thereby killing the bacteria. *n*-Heptyl (C7) amino 15 and its analogue 14, in the absence of *E. coli*, emit significant fluorescence, presumably due to the entry of the probe into the cyclodextrin cavity. Interestingly, *n*-pentyl- and other C5-amino derivatives (5–7) induced large changes in fluorescence, comparable to those induced by the C6 derivatives. This finding is contrary to our finding that these C5 derivatives had lower antibacterial activity against *E. coli* than did the C6 derivatives. Presumably, the C5 derivatives interact with an outer membrane and perturb it but cannot enter the cytoplasm due to their lower hydrophobicity than the C6 derivatives.

**Potential of Antibiotics by Co-Treatment with Cyclodextrin Derivatives via Outer Membrane Disruption in Gram-Negative Bacteria.** We investigated the outer membrane damage induced by C5-amino derivatives

when combined with other antibiotics. Erythromycin is a well-known macrolide antibiotic that inhibits protein synthesis by binding to the bacterial rRNA complex. Novobiocin is an aminocoumarin antibiotic that acts by inhibiting bacterial DNA gyrase. Because these antibiotics cannot reach their intracellular targets due to the outer membrane barrier, they are ineffective on Gram-negative bacteria. However, we observed that combining these conventional antibiotics with pentylamino cyclodextrins 4–7 increased their antibacterial activity against *E. coli* (Figure 6). Co-treatment with cyclo-

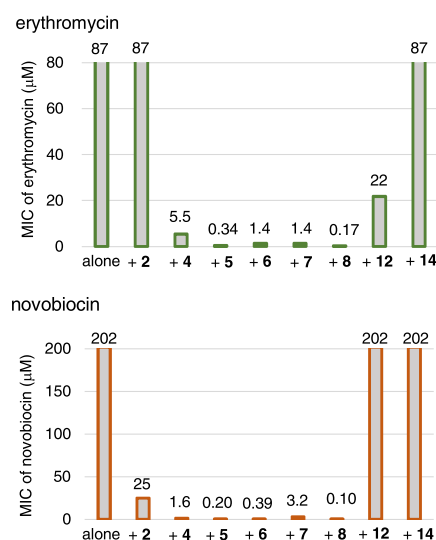


**Figure 6.** Potentiation of erythromycin and novobiocin in *E. coli* by alkylamino cyclodextrins. The concentration of cyclodextrin was a quarter of the MIC of each cyclodextrin.

dextrin 7 (2  $\mu\text{M}$ , 25% MIC) decreased the MIC of erythromycin from 87 to 1.4  $\mu\text{M}$  and that of novobiocin from 202 to 3.2  $\mu\text{M}$ . 3-Methylbutyl 5 (4  $\mu\text{M}$ , 25% of its MIC) decreased their MIC values to 0.34 and 0.20  $\mu\text{M}$ , respectively. The C6 derivative cyclopentylmethyl 8 (4  $\mu\text{M}$ , 25% MIC) reduced the MIC of erythromycin to 0.17  $\mu\text{M}$  and that of novobiocin to 0.10  $\mu\text{M}$ . Fractional inhibitory concentration index (FICI) values<sup>26</sup> of 5, 7, and 8 with erythromycin were 0.25, 0.27, and 0.25, respectively, and those with novobiocin were the same, suggesting that all of them were synergistic with the antibiotics. These results clearly demonstrate that the cyclodextrin disrupts the outer membrane barrier, allowing erythromycin and novobiocin to enter and access their targets.

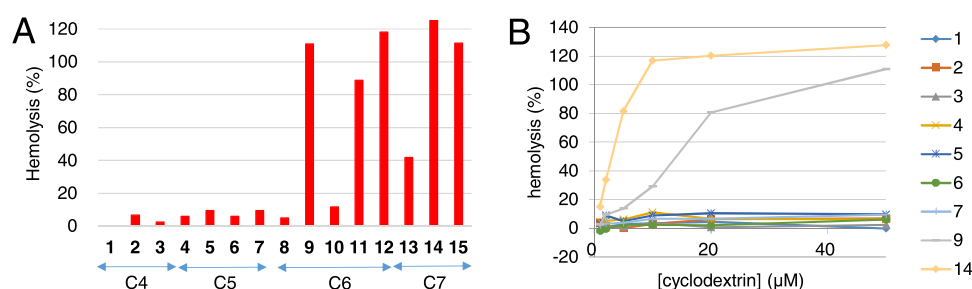


**Figure 7.** Hemolytic activity of alkylamino cyclodextrins ((A) [cyclodextrin] = 50  $\mu\text{M}$ , (B) dose-dependent curves of 1–7, 9, and 14). Rabbit red blood cells were incubated with a cyclodextrin at 37  $^{\circ}\text{C}$ , and hemolysis was estimated by measuring the absorbance at 540 nm. Lysolecithin (50  $\mu\text{M}$ ) was used to determine 100% hemolysis level.

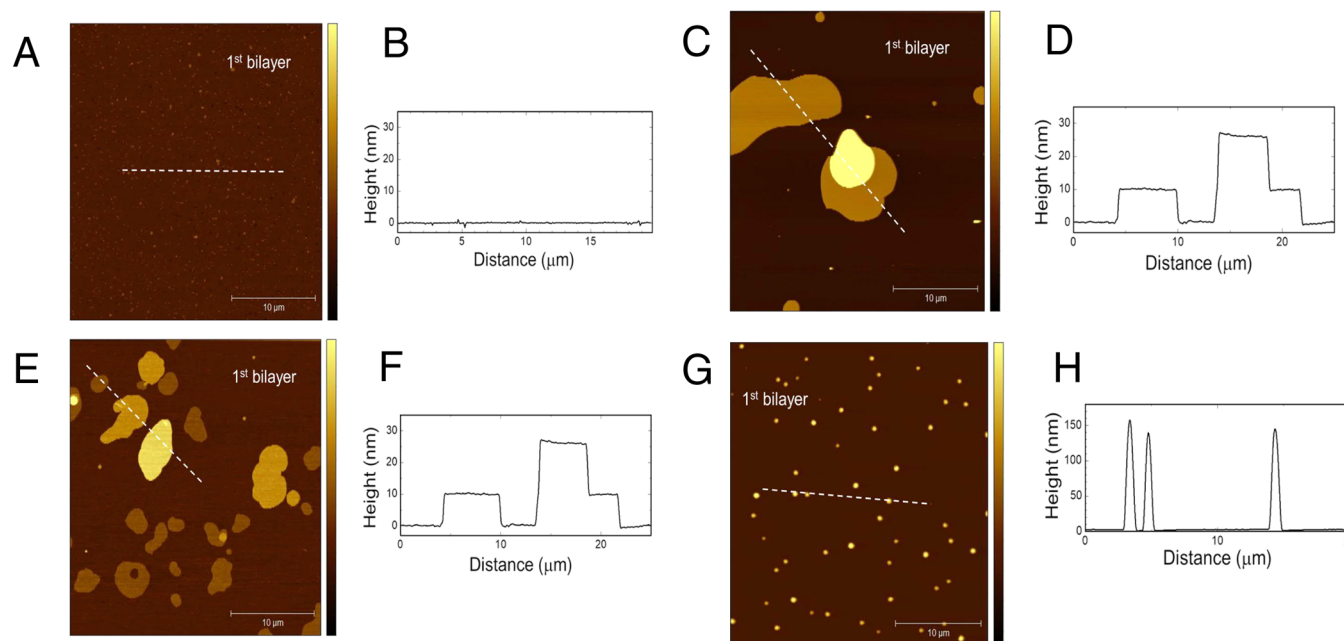


**Figure 8.** Structural changes of planar lipid bilayers caused by antibacterial agents. DOPG bilayers interact with a native cyclodextrin (A, B), 2-ethylbutylamino cyclodextrin 10 (C, D), polymyxin B (E, F), and melittin (G, H). Height profiles (B, D, F, H) along dashed lines in (A, C, E, and G), respectively. Z scale: 25 nm for (A, C, and E), 200 nm for (G). The lipid bilayers were incubated with antibacterial agents; (10  $\mu\text{g mL}^{-1}$ ) for 30–60 min before AFM observation.

Schweizer reported homodimeric tobramycin as an excellent antibiotic adjuvant to allow the use of lower doses of novobiocin.<sup>27</sup> The 2000-fold potentiation of novobiocin antibacterial activity by derivative 5 is comparable to that induced by the tobramycin homodimer. While erythromycin and novobiocin are not effective alone against Gram-negative pathogens, these results suggest that they may be effective when used in combination with these cyclodextrins.

#### Assessment of Cyclodextrin Toxicity in Animal Cells.

The toxicity of cyclodextrins against rabbit red blood cell was investigated via hemolysis assay. The butyl (C4)- and pentyl (C5)-modified amino cyclodextrins 1–7 exhibited low hemolysis (Figure 7; Table S1). The hemolytic properties of the hexyl (C6) analogues varied: cyclopentylmethyl 8 and 2-ethylbutyl 10 showed lower hemolytic activity (5 and 12% at 50  $\mu\text{M}$ ), while that of 4-methylpentyl 9, 2-methylpentyl 11, and *n*-hexyl 12 was high (>80% at 50  $\mu\text{M}$ ). Of the heptyl (C7) analogues, the hemolytic activity of cyclohexane-containing 13 was moderate (42%) compared to that of the branched 14 and linear 15 derivatives (>100%). The  $\text{ED}_{50}$  values, concentrations giving 50% hemolysis, of 1–7 were given as >50  $\mu\text{M}$  because of their low hemolysis and those of 9 and 14 were 14

and 3  $\mu\text{M}$ , respectively, while the values of antimicrobial peptides melittin and gramicidin S were 0.2–0.5 and 10  $\mu\text{M}$ , respectively.<sup>28</sup> Roughly speaking, the cyclodextrins that were active against Gram-negative bacteria (Figure 1) exhibited relatively high hemolytic activity, while those with antibacterial activity only against Gram-positive bacteria had low hemolytic activity. The membranes of Gram-positive *S. aureus* are rich in the anionic lipids phosphatidylglycerol and cardiolipin, while Gram-negative *E. coli* have a higher abundance of “neutral” phosphatidylethanolamine.<sup>29</sup> Phosphatidylethanolamine and phosphatidylcholine are abundant in red blood cells.<sup>30</sup> Therefore, the relatively hydrophilic (cationic) cyclodextrins 3–7 demonstrated more effective against Gram-positive bacteria than Gram-negative bacteria and the relatively hydrophobic cyclodextrins such as 3-methylhexyl 14 demonstrated higher hemolytic activity and antibacterial activity against Gram-negative bacteria. It should be also noted here that several cyclodextrins were more active against certain bacteria. For example, 2-methylpentyl 11 exhibited strong activity against *E. coli* and *P. aeruginosa* but low activity against *S. Typhimurium*. It may be due to differences in bacterial cell membrane and lipid molecules. The membrane of *P. aeruginosa*

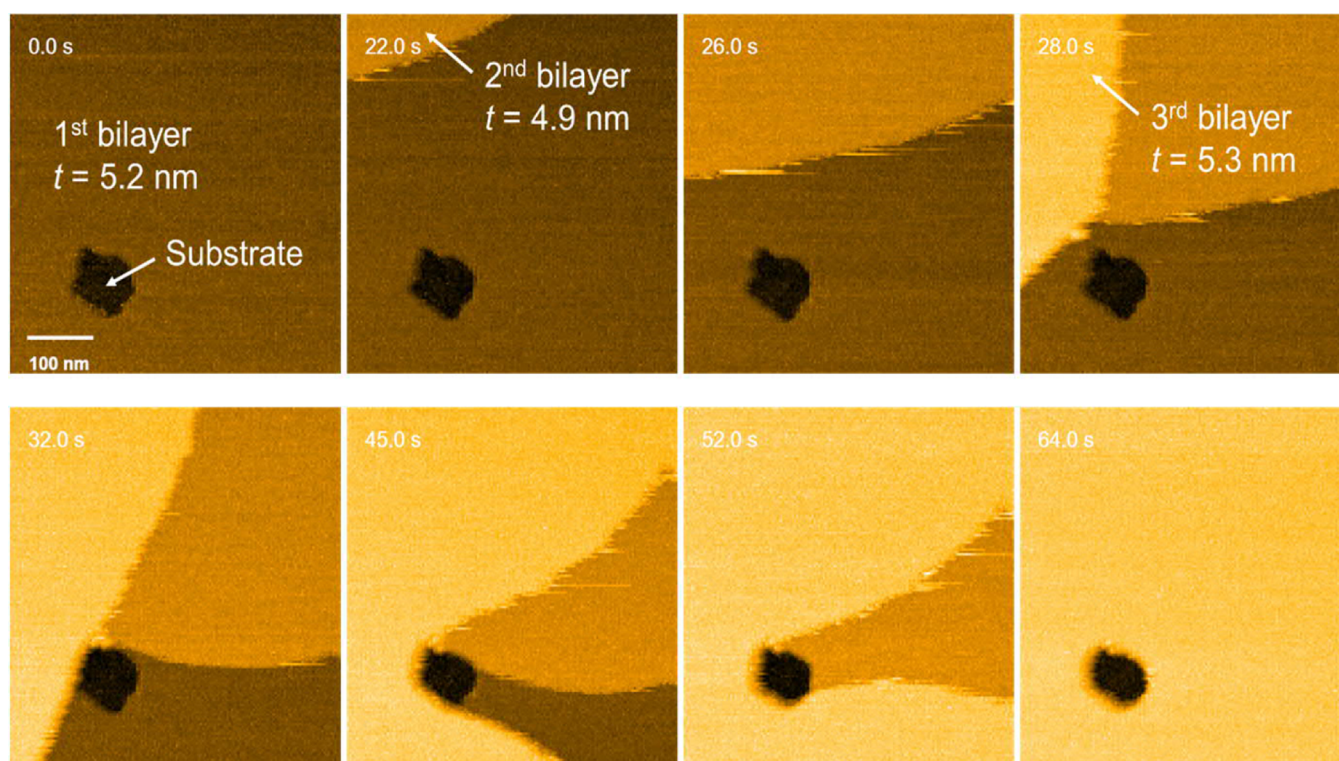


**Figure 9.** Snapshots of a high-speed AFM movie capturing the growth of a multilayered structure caused by 2-ethylbutylamino cyclodextrin **10**. Surfaces of substrate, first bilayer, second bilayer, and third bilayer are indicated by arrows with its thickness ( $t$ ). Frame rate: 1 frame/s. The snapshots started about 2 min after the addition of the alkylamino cyclodextrin **10**. Note that 0 s is the starting time of the movie, not the timing of cyclodextrin addition.

has a higher abundance of phosphatidylethanolamine than that of *E. coli*.<sup>29</sup> The bacteria also have characteristic outer membrane containing lipopolysaccharides outside the cytoplasmic membrane. Either or both differences may be the reason for the observed antibacterial activity. From this perspective, the finding that ethylbutyl **10** had low hemolytic activity (12%) and high antibacterial activity against both Gram-negative and Gram-positive bacteria (MIC: *E. coli*, 4.5  $\mu$ M; *S. aureus*, 2.3  $\mu$ M) seems unique. Chapman and Gellman reported that amphiphilic balance is one of the most important features of antimicrobial polymer chemistry, but that stereochemistry also affects antibacterial and hemolytic activity.<sup>31</sup> Subunit stereochemistry affects the shape of polymer chains, thereby affecting their biological activity. In the case of the ethylbutylamino **10**, the cyclodextrin molecular structure is relatively rigid due to inter-residue hydrogen bonds within the molecule; thus, a drastic shape change in this oligomer seems impossible. However, the highly branched structure of the ethylbutyl groups, which differs slightly from those of other C6 alkyl groups, may lead to unique local interactions with membranes that confer differential molecular behavior that is less disruptive toward animal cells. Fine-tuning of functional groups on a cyclodextrin molecule may produce cyclodextrin derivatives that react differently with the membranes of bacterial and mammalian cells. Interestingly, the derivatives with low hemolytic activity (5, 7, and 8) are those that potentiated the effects of the combined antibiotics (hemolysis at 50  $\mu$ M: **10**, 9, and 5%, respectively). Few compounds selectively permeabilize the bacterial outer membrane, as exemplified by the side effects of colistin and polymyxin B, agents used to treat Gram-negative bacterial infections. Cyclodextrins might selectively permeabilize bacterial mem-

branes such that they could be used to safely revitalize the effectiveness of conventional antibiotics to treat resistant strains of bacteria.

**Atomic Force Microscopy (AFM) Imaging of Lipid Bilayer Disturbance as a Bacterial Cytoplasmic Membrane Model.** Cyclodextrin-induced structural changes in bacterial membranes were observed directly using atomic force microscopy (AFM). The thick peptidoglycan layer of Gram-positive bacteria confounds direct observation of membrane changes using AFM. Therefore, in place of a bacterial cell membrane, we investigated structural changes in a model lipid bilayer membrane (Figure 8). As a model of the *S. aureus* cytoplasmic membrane, we used an artificial planar lipid bilayer of 1,2-dioleoyl-*sn*-glycero-3-phospho-*rac*-(1-glycerol) (DOPG) bilayer, as the bacterial membrane is rich in negatively charged lipids (PG, 58%; cardiolipin (diphosphatidyl glycerol), 42%).<sup>29</sup> The cyclodextrin used in these experiments was 2-ethylbutylamino derivative **10**, which showed high antibacterial activity and low hemolytic activity. Before the addition of cyclodextrin, the DOPG bilayers were flat, without holes or protrusions. Treatment with the control (native [unmodified] cyclodextrin with no antibacterial activity) caused no structural changes (Figure 8A,B). After the interaction with cyclodextrin **10**, a “multistep” structure was observed (Figure 8C,D), indicating that the alkylamino moiety of **10** facilitated interaction with the DOPG bilayer. The observed step sizes were 10 and 15 nm (Figure 8D). Because the thickness of one bilayer is 4–5 nm, these heights correspond to the thickness of two and three bilayers, indicating a multilayered structure. Similarly, polymyxin B,<sup>11</sup> an amphiphilic antimicrobial cyclic peptide, induced a multilayered structure (Figure 8E,F). In contrast, melittin,<sup>21</sup> an antibacterial linear  $\alpha$ -helical peptide,



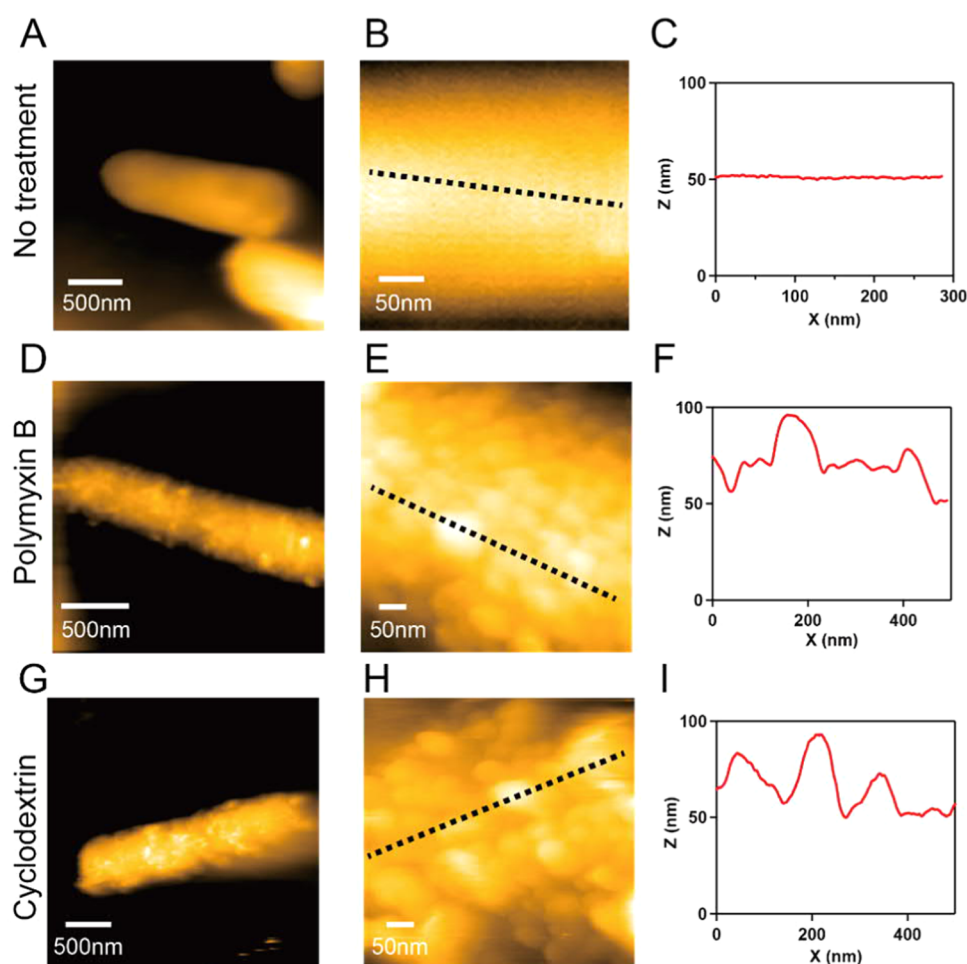


**Figure 10.** Structural changes of bacterial cell surface caused by antimicrobial reagents. (A) Bacterial cell before the addition of antimicrobial reagents. (B) Highly magnified AFM image of cell surface before the addition of antimicrobial reagents. (D) Bacterial cell after the addition of polymyxin B. (E) Highly magnified AFM image after the addition of polymyxin B. (G) Bacterial cell after the addition of 2-ethylbutylamino cyclodextrin 10. (H) Highly magnified AFM image after the addition of cyclodextrin. (C, F, I) Cross-sectional profiles corresponding to dotted lines in (B), (E), and (H). As antimicrobial reagents,  $100 \mu\text{g mL}^{-1}$  of polymyxin B and  $100 \mu\text{g mL}^{-1}$  of the cyclodextrin were, respectively, applied on the sample stage and then the sample was incubated for 4 h in polymyxin B or 5 h in the cyclodextrin.

did not induce a multilayered structure but rather many “particles” with heights of several hundred nanometers (Figure 8G,H). The area or number of multilayered structures and particles increased with increasing concentrations of the antibacterial agents (Figure S1). In the partially formed DOPG bilayer, used for observation, the space between the bilayer islands decreased after interaction with the cyclodextrins (Figure S2). These results indicate that the cyclodextrins were incorporated into the DOPG bilayer. Such structural changes did not occur in a cell membrane model made of a neutral 1,2-dioleoyl-*sn*-glycero-3-phosphocholine (DOPC) bilayer (Figure S3) using PC as one of the major lipids in a mammalian cell membrane.<sup>30</sup> The results are coincident with the observed low hemolytic activity of cyclodextrin 10. These results suggest that the electrostatic interaction between the negatively charged membrane bilayer and the positively charged antibacterial cyclodextrin is essential for the membrane structural changes observed here. Thus, the cyclodextrin derivatives may discriminate between bacterial and mammalian cell membranes.

We observed the dynamic process of alkylamino cyclodextrin-induced structural changes in the lipid bilayer using high-speed (HS)-AFM. Figure 9 shows HS-AFM snapshots

about 2 min after the addition of 2-ethylbutylamino cyclodextrin 10. The image at 0 s shows a single lipid bilayer (thickness, 5.2 nm) with a small defect. After 22 s, a second bilayer (thickness, 4.9 nm) appeared and grew in area (26 s). At 28 s, the third bilayer (thickness, 5.3 nm) appeared and grew over time (32, 45 s), merged with the second bilayer (52 s), and finally filled the imaging area (64 s). Interestingly, the second and third bilayers did not cover over the defect in the bilayer, suggesting that bilayer–bilayer interaction facilitates growth of the multilayered structure. To the best of our knowledge, the observation of such structural change in lipid bilayers by real-time HS-AFM imaging has not been reported previously. This incorporation of the agent and the formation of multilayered structures in the cytoplasmic membrane of bacterial cells disrupt the bacterial membrane integrity, leading to cell death. The observed multilayered structure clearly differed from the “particle” structure produced by melittin that is thought to act through a “toroidal pore” model.<sup>21</sup> Thus, the interaction between the cyclodextrin derivative and bacterial membrane differs from that of the toroidal pore model. Instead, the interaction may be similar to that of polymyxin B, the mechanism of which has not been confirmed. The bilayer–bilayer interaction induced by cyclodextrin may be similar to



that induced by polymyxin B, which mediates the contacts between the inner and outer membranes that has been proposed as an alternative mechanism of action by polymyxin B.<sup>11</sup> This elucidation of the cyclodextrin-induced structure may provide clues for understanding the mechanism of action of polymyxin B.

### AFM Imaging of Cyclodextrin-Induced Outer Membrane Disruption in Gram-Negative Bacteria In Vivo.

Cyclodextrin-induced structural changes in the *E. coli* cell surface were observed in live *E. coli* in physiological solution using HS-AFM (Figure 10A).<sup>32,33</sup> A magnified AFM image of a bacterial cell before the addition of the antimicrobial reagent shows a smooth surface over an area of several hundred nanometers (Figure 10B,C). The morphology of the cell changed drastically after the addition of the antimicrobial peptide polymyxin B (Figure 10D), adopting a rough surface structure with height differences of several dozen nanometers (Figure 10E,F). Such structural changes were observed over the entire cell surface. Similar morphological changes were observed after the addition of 2-ethylbutylamino cyclodextrin 10 (Figure 10G–I), with a rough surface structure characterized by structural undulations in amplitude of over several dozen nanometers (Figure 10H,I), a thickness greater than that of the outer membrane of Gram-negative bacteria.<sup>34</sup> These drastic changes in structure suggest that the outer bacterial membrane was damaged by these antimicrobial reagents. A previous AFM study showed that polymyxin B and its analogue led to lethal membrane damage in Gram-negative bacteria.<sup>35,36</sup> Our study is the first to report imaging evidence in live bacteria of the outer membrane damage caused by cyclodextrins, providing direct proof that cyclodextrins disrupt this membrane. These findings clearly demonstrate at nanometer resolution that AFM has the potential for novel pharmacological applications.

## CONCLUSIONS

This investigation of  $\gamma$ -cyclodextrin derivatives modified with a variety of alkylamino substituents shows that these agents have strong antibacterial activity, equivalent to that of natural antibiotic peptides. The number of carbon atoms in the alkylamino group correlates with the cyclodextrin activity, and the shape of the alkyl moiety may have some influence as well, which demonstrates that the activity of the cyclodextrin derivatives may be tuned as desired. Most of the cyclodextrins examined here demonstrated high activity against Gram-positive *S. aureus*, including MRSA, and several were active against Gram-negative bacteria, including extended-spectrum  $\beta$ -lactamase-producing *E. coli* and carbapenemase-producing *K. pneumoniae*. The activity of these cyclodextrin derivatives may be specific to bacterial cell membranes, which could lead to the development of similar agents with selective activity against bacteria. Several lines of evidence, including direct visualization using AFM, clearly indicate that these derivatives act through disruption of the bacterial cell membrane. Because the acquisition of resistance to membrane-disrupting processes is difficult, the results suggest that cyclodextrin derivatives may be promising agents for use in treating drug-resistant Gram-positive and Gram-negative bacteria. Our evidence also indicates that cyclodextrins may be promising as potentiators or enhancers of other antibiotics to combat drug-resistant pathogens. While the activity of these cyclodextrin derivatives is not superior to that of antibiotic peptides, the versatility of cyclodextrin derivatization may allow for the rational design of

molecules with desired novel activities and the revitalization of resistance-acquired conventional drugs.

## EXPERIMENTAL SECTION

**General Synthetic Chemistry.** <sup>1</sup>H spectra were recorded at 30 °C on a Bruker AVANCE400Plus Nanobay and AVANCE500US CryoProbe. MALDI-TOF mass measurements were carried out with a JEOL JMS-S3000 spectrometer. A microwave reactor was a Biotage Initiator EXP used for the Huisgen reaction. All compounds were determined to be pure by elemental analysis performed with Elementar vario EL cube.

### General Procedure for the Synthesis of *N*-Alkyl-Boc-propargylamines for the Preparation of Cyclodextrins.

*N*-3-Methylhexyl-Boc-propargylamine was prepared as follows. Boc-propargylamine (201 mg,  $1.30 \times 10^{-3}$  mol) was stirred with 55% NaH (115 mg,  $2.64 \times 10^{-3}$  mol of NaH) in DMF (6 mL) for 30 min under argon. After the addition of 3-methylhexyl mesylate (498 mg,  $2.57 \times 10^{-3}$  mol), the reaction mixture was stirred for 3 h. After the addition of a small amount of methanol and then EtOAc, the reaction mixture was washed with water and saturated aq. NaCl. It was dried with anhydrous Na<sub>2</sub>SO<sub>4</sub> and concentrated in vacuo. Silica gel chromatography (hexane/AcOEt) yielded the corresponding alkyne as oil (248 mg, 75.3%). The other derivatives were prepared as reported previously.<sup>17,19</sup>

### General Procedure for the Synthesis of Cyclodextrins.

The preparation of 3-methylhexylamino-modified 14 was described. The other derivatives were prepared as reported previously.<sup>16,17</sup> (3-methylhexyl-aminocyclodextrin (14)). A reaction solution was prepared by dissolving per-2,3-acetylated  $\gamma$ -cyclodextrin octaazide 16 (50.7 mg,  $2.34 \times 10^{-5}$  mol) in DMSO–H<sub>2</sub>O (5:1) (4.8 mL) containing *N*-3-methylhexyl-Boc-propargylamine (55.1 mg, 1.16 mol equiv to an azide group), CuSO<sub>4</sub> 5H<sub>2</sub>O (4.72 mg, 0.1 mol equiv), and sodium ascorbate (46.7 mg, 1.25 mol equiv). After MW heating (120 °C, 30 min), ethyl acetate was added followed by washing with 5% aq. EDTA. Silica gel column chromatography (CH<sub>2</sub>Cl<sub>2</sub>/methanol) gave the click reaction product (74.3 mg). Deprotection of acetyl groups with NaOMe–MeOH followed by that of the Boc group with TFA gave the desired product 14 (66.3%, overall yield): proton nuclear magnetic resonance (<sup>1</sup>HNMR) (400 MHz, DMSO-*d*<sub>6</sub>):  $\delta$  0.80–0.87 (48H, CH<sub>3</sub>–), 1.08–1.10 (8H, CH<sub>3</sub>–CH<sub>2</sub>–CH<sub>2</sub>–), 1.17–1.30 (24H, CH<sub>3</sub>–CH<sub>2</sub>–CH<sub>2</sub>–), 1.37–1.42 (16H, –CH(CH<sub>3</sub>)–CH<sub>2</sub>–CH<sub>2</sub>–NH–), 1.58–1.61 (8H, –CH<sub>2</sub>–CH<sub>2</sub>–NH–), 2.92 (16H, –CH<sub>2</sub>–NH–), 3.22–3.30 (16H, cyclodextrin -2,4), 3.67 (8H, cyclodextrin -3), 4.09 (24H, cyclodextrin -5, –NH–CH<sub>2</sub>–triazole), 4.44–4.48 (16H, cyclodextrin -6), 5.10 (8H, cyclodextrin-1), 6.09 (18H, OH), 8.06 (7H, triazole), 9.17 (14H, –NH<sub>2</sub><sup>+</sup>–), <sup>13</sup>CNMR (100 MHz, DMSO-*d*<sub>6</sub>):  $\delta$  14.48, 19.49 (CH<sub>3</sub>–), 19.75 (CH<sub>3</sub>–CH<sub>2</sub>–), 30.19 (–CH–(CH<sub>3</sub>)–), 32.58 (–CH<sub>2</sub>–CH<sub>2</sub>–NH–), 38.78 (CH<sub>3</sub>–CH<sub>2</sub>–CH<sub>2</sub>–), 41.39 (N–CH<sub>2</sub>–triazole), 45.18 (–CH<sub>2</sub>–NH–), 49.98 (cyclodextrin-6), 69.89 (cyclodextrin-5), 72.24, 72.57 (cyclodextrin-2,3), 82.18 (cyclodextrin-4), 101.94 (cyclodextrin-1), 127.42 (CHtriazole), 138.72 (Ctriazole), Found: C, 46.20; H, 6.60; N, 11.59%. Calcd for C<sub>128</sub>H<sub>200</sub>N<sub>32</sub>O<sub>32</sub> + 7.0H<sub>2</sub>O + 8.1TFA: C, 45.90; H, 6.57; N, 11.88%.

**Bacteria and Minimum Inhibitory Concentration (MIC).** The drug-sensitive microorganisms were *S. aureus* cells FDA 209P, *B. subtilis* ATCC 663, *E. coli* K12 W3110, *S. Typhimurium* LT2, and *P. aeruginosa* PAO1. Their MICs were

determined by the liquid microdilution method, using serially diluted (twofold) cyclodextrins. The cells ( $1 \times 10^4$ ) were cultured at 37 °C for 20 h in a Mueller Hinton broth (0.1 mL) containing cyclodextrin in a 96-well microtiter plate. The MIC was determined as the lowest concentration of cyclodextrin at which cells were unable to grow.

The strains of MIC experiment against drug-resistant bacteria used were as follows: *S. aureus* ATCC 29213 and methicillin-resistant *S. aureus* clinical strain (K11), *E. coli* ATCC 25922, expanded spectrum  $\beta$ -lactamase-producing *E. coli* clinical strain (I25), carbapenemase-producing *E. coli* clinical strain (M11), carbapenemase-producing *K. pneumoniae* ATCC BAA-1705, *K. pneumoniae* ATCC BAA-1706, *P. aeruginosa* ATCC 27853, carbapenemase-producing *P. aeruginosa* clinical strain (S11), and carbapenemase-producing *P. aeruginosa* clinical strain (S27). We measured by minimum inhibitory concentrations with the broth microdilution susceptibility test in accordance with Clinical and Laboratory Standards Institute M 100-S29.<sup>37</sup> The agents were prepared by twofold dilutions in Mueller Hinton II broth (cation-adjusted, BD) on each plate. The colonies were suspended in the broth and the microbial suspension standardized to an optical density of McFarland 0.5. The suspension was diluted to 1:10 and transferred 5  $\mu$ L to each well. The wells were mixed, and each plate was incubated under suitable conditions depending on the following bacteria, typically for 16–24 h at 35 °C. MIC values were determined as the lowest antibiotic concentration that inhibited microbial growth.

**K<sup>+</sup> Efflux and Cell Viability.** Bacterial cells were washed twice with the buffer (100 mM choline chloride/50 mM Mops-Tris, pH 7.2) and suspended in this buffer at  $2 \times 10^9$  cells cm<sup>-3</sup>. The final volume of the cell suspension was 1 mL. The cells were incubated with cyclodextrin at 37 °C for 30 min. After incubation, 0.1 mL of the cell suspension was taken, diluted with physiological saline, and dispersed on an agar plate prepared with 1% polypeptone, 0.5% yeast extract, 0.5% NaCl, and 1.5% agar (pH was adjusted by adding 1 M NaOH). The colonies were counted after standing overnight at 37 °C, and the viability of the cells was determined. The remaining cell suspension was centrifuged, and the amount of K<sup>+</sup> in the supernatant was measured using a K<sup>+</sup>-selective electrode. Melittin (10  $\mu$ M) and polymyxin B (200  $\mu$ g mL<sup>-1</sup>) were used to determine the 100% level of K<sup>+</sup> efflux from *S. aureus* and *E. coli*, respectively.

**Cytoplasmic Membrane Depolarization Assay.** The depolarization of the cytoplasmic membrane of *S. aureus* by cyclodextrins was determined using the membrane potential-sensitive dye DiSC<sub>3</sub>5. The bacteria were washed and resuspended in 5 mM HEPES/5 mM glucose/100 mM KCl buffer (pH 7.2) to OD<sub>650</sub> = 0.05. This cell suspension was incubated with 0.5  $\mu$ M DiSC<sub>3</sub>5 for 10 min for a stable reduction in fluorescence due to DiSC<sub>3</sub>5 uptake and quenching in the cell in response to an intact membrane potential. 96-Well plates were used, and each cyclodextrin (final concentration = 1  $\mu$ M) in the buffer (100  $\mu$ L) was then mixed with the cell suspension of *S. aureus* (100  $\mu$ L) and fluorescence was monitored for 10 min in a Corona grating microplate reader SH-9000Lab at an excitation wavelength of 622 nm and an emission wavelength of 670 nm. Melittin (final concentration = 1  $\mu$ M) was used as a positive control.

**Outer Membrane Permeabilization Assay.** 96-Well plates were used, and the fluorescence was recorded with a Corona grating microplate reader SH-9000Lab. *E. coli* was

washed and resuspended in 5 mM sodium N-(2-hydroxyethyl)piperazine-N'-ethanesulfonic acid (HEPES) buffer (pH 7.2) to obtain absorbance at 650 nm of 0.4. Each cyclodextrin in the buffer (90  $\mu$ L) was then mixed with the cell suspension of *E. coli* (100  $\mu$ L) and NPN (10  $\mu$ L). The final concentrations of butyl (1–3), pentyl (4–7), hexyl (8–12), and heptyl (13–15) amino cyclodextrins were 20, 19, 18, and 18  $\mu$ M, respectively, and the final concentration of NPN was 10  $\mu$ M. Changes in fluorescence were recorded for 31 min using excitation and emission wavelengths of 340 and 410 nm, respectively. Polymyxin B (final concentration = 1  $\mu$ M) was used as a positive control.

**Potential of Combined Antibiotics against Gram-Negative Bacteria.** Each of the cyclodextrins was tested for its ability to potentiate the combined antibiotics (erythromycin and novobiocin). The MIC of the antibiotics supplemented with the cyclodextrin (at 25% of cyclodextrin's MIC to avoid a direct effect on bacteria) was determined as described above and compared to the MIC of the antibiotic alone.

**Hemolytic Activity.** Rabbit erythrocytes obtained from rabbit blood (Nippon Bio-Test Laboratories, Inc.) were suspended in buffer (150 mM NaCl/10 mM Hepes-NaOH, pH 7.4) at a final concentration of 0.5% hematocrit. After incubation with cyclodextrins at 37 °C for 30 min, hemolysis was estimated by measuring the absorbance at 540 nm. Lysolethicin (50  $\mu$ M) was used to determine the 100% level of hemolysis.

**AFM Observation of Artificial Lipid Bilayer Change Caused by Antimicrobial Reagents.** A chloroform solution of 1,2-dioleoyl-*sn*-glycero-3-phospho-*rac*-(1-glycerol) (DOPG) or 1,2-dioleoyl-*sn*-glycero-3-phosphocholine (DOPC) in a glass vial was dried under nitrogen stream and placed in vacuum for over 2 h to form lipid film. The lipid film was hydrated by phosphate-buffered saline (PBS) (pH 7.4) at room temperature, forming a liposomal suspension. The liposomal suspension was sonicated for 10 s to downsize the liposomes. To form DOPG-supported lipid bilayer on mica surface, the mica surface was coated by 0.1 vol % 3-aminopropyltriethoxysilane (APTES) solution for 5 min and then rinsed by pure water. To the APTES-coated mica, 5 mg/mL DOPG liposome suspension was applied, incubated for 5 min, and then rinsed by PBS to remove remaining liposomes. The PBS solution over the DOPG bilayer was replaced by an antimicrobial reagent solution (10  $\mu$ g mL<sup>-1</sup>) and incubated for 30–60 min before AFM observation. For high-speed AFM (HS-AFM) observation, the incubation time was about 2 min. AFM images were taken in PBS solutions with antimicrobial reagents. The AFM instrument and cantilever used for taking static images were Cypher (Oxford instruments) and BL-AC40TS (Olympus), respectively. For HS-AFM measurement, we used laboratory-built HS-AFM<sup>38</sup> and cantilever AC10 (Olympus) with electron beam deposition tip.<sup>39</sup>

**AFM Observation of a Living *E. coli* Cell Treated with Antimicrobial Reagents.** *E. coli* cells were cultured in LB liquid media and grown at 37 °C with shaking until they reached log phase. For AFM observation, bacterial cells were collected by centrifugation at 8000g for 5 min at room temperature. The bacterial pellet was resuspended in 200  $\mu$ L of PBS. AFM imaging was performed with a laboratory-built high-speed AFM (HS-AFM) as reported previously.<sup>32</sup> The HS-AFM was equipped with small cantilevers ( $k = 0.1$  N/m,  $f = 800$ –1200 kHz in water) and operated in the tapping mode. The AFM styli were grown on each cantilever by electron

beam deposition. The mica substrate for the AFM observation of bacterial cell was prepared by the method same as reported previously.<sup>32</sup> The *E. coli* cell suspension was loaded on the treated mica in PBS. After 30 min, the sample was gently rinsed with fresh PBS. For such condition, it has been confirmed that bacterial cells were alive on the treated mica as reported previously.<sup>32,33</sup> As antimicrobial reagents, polymyxin B of 100  $\mu\text{g mL}^{-1}$  or cyclodextrin of 100  $\mu\text{g mL}^{-1}$  were, respectively, applied on the sample stage and then the sample was incubated for 4 h in polymyxin B or 5 h in cyclodextrin. After each incubation, the sample was gently rinsed with fresh PBS and measured in PBS.

## ■ ASSOCIATED CONTENT

### Supporting Information

The Supporting Information is available free of charge at <https://pubs.acs.org/doi/10.1021/acsomega.1c04541>.

Values of MIC and hemolysis (Tables S1 and S2) and AFM observation (Figures S1–S3) (PDF)

## ■ AUTHOR INFORMATION

### Corresponding Author

Hatsuo Yamamura – Graduate School of Engineering, Nagoya Institute of Technology, Nagoya 466-8555, Japan;  
orcid.org/0000-0003-3137-6230;  
Email: [yamamura.hatsuo@nitech.ac.jp](mailto:yamamura.hatsuo@nitech.ac.jp)

### Authors

Tatsuya Hagiwara – Graduate School of Engineering, Nagoya Institute of Technology, Nagoya 466-8555, Japan

Yuma Hayashi – Graduate School of Engineering, Nagoya Institute of Technology, Nagoya 466-8555, Japan

Kayo Osawa – Department of Medical Technology, Faculty of Health Sciences, Kobe Tokiwa University, Kobe 653-0838, Japan

Hisato Kato – Graduate School of Clinical Pharmacy, Shujitsu University, Okayama 703-8516, Japan

Takashi Katsu – Graduate School of Clinical Pharmacy, Shujitsu University, Okayama 703-8516, Japan

Kazufumi Masuda – Graduate School of Clinical Pharmacy, Shujitsu University, Okayama 703-8516, Japan

Ayumi Sumino – Nano Life Science Institute (WPI-NanoLSI), Kanazawa University, Kanazawa 920-1192, Japan; Institute for Frontier Science Initiative, Kanazawa University, Kanazawa 920-1192, Japan

Hayato Yamashita – Graduate School of Engineering Science, Osaka University, Toyonaka, Osaka 560-8531, Japan

Ryo Jinno – Graduate School of Engineering Science, Osaka University, Toyonaka, Osaka 560-8531, Japan

Masayuki Abe – Graduate School of Engineering Science, Osaka University, Toyonaka, Osaka 560-8531, Japan;  
orcid.org/0000-0001-5619-3911

Atsushi Miyagawa – Graduate School of Engineering, Nagoya Institute of Technology, Nagoya 466-8555, Japan;  
orcid.org/0000-0003-0809-0912

Complete contact information is available at:  
<https://pubs.acs.org/doi/10.1021/acsomega.1c04541>

### Author Contributions

The study was designed by H.Y. The synthetic work and characterization of compounds was conducted by H.Y., T.H., Y.H., and A.M. Antibacterial activity (MIC) assay was

conducted by T.H., Y.H., and K.Y. In vitro assays of bacterial  $\text{K}^+$  efflux and cell viability were performed by H.K., T.K., and K.M. Cytoplasmic membrane depolarization assay, outer membrane permeabilization assay, and hemolytic activity assay were conducted by T.H. Potentiation assay was performed by Y.H. AFM observation was performed by A.S., H.Y., R.J., and M.A. All authors gave approval to the final version.

### Notes

The authors declare no competing financial interest.

## ■ ACKNOWLEDGMENTS

The authors thank MARUZEN-YUSHODO Co., Ltd. for the English language editing. This work was supported by JSPS Grants-in-Aid for Scientific Research grant nos. 15K07857 (H.Y.), 19H05789 (M.A.), and 20H03223 (H.Y.) and Japan Science and Technology Agency JPMJPR15FD (H.Y.). The authors thank Yuki Sugiyama, Miho Nonaka, Takahiro Mabuchi, Shinya Ohno, and Tomoki Ishida for assistance of synthetic and bacterial experiments.

## ■ REFERENCES

- (1) *Antimicrobial resistance: Global report on surveillance*; WHO, 2014.
- (2) Zavascki, A. P.; Goldani, L. Z.; Li, J.; Nation, R. L. Polymyxin B for the treatment of multidrug-resistant pathogens: a critical review. *J. Antimicrob. Chemother.* **2007**, *60*, 1206–1215.
- (3) Hancock, R. E. W.; Sahl, H.-G. Antimicrobial and host-defense peptides as new anti-infective therapeutic strategies. *Nat. Biotechnol.* **2006**, *24*, 1551–1557.
- (4) Van Bambeke, F.; Mingeot-Leclercq, M.-P.; Struelens, M. J.; Tulkens, P. M. The bacterial envelope as a target for novel anti-MRSA antibiotics. *Trends Pharmacol. Sci.* **2008**, *29*, 124–134.
- (5) Lohner, K.; Hilpert, K. Antimicrobial peptides, cell membrane and microbial surface interaction. *Biochim. Biophys. Acta* **2016**, *1858*, 915–917.
- (6) Wimley, W. C. Describing the mechanism of antimicrobial peptide action with the interfacial activity model. *ACS Chem. Biol.* **2010**, *5*, 905–917.
- (7) Herzog, I. M.; Fridman, M. Design and synthesis of membrane-targeting antibiotics: from peptides- to aminosugar-based antimicrobial cationic amphiphiles. *Med. Chem. Commun.* **2014**, *5*, 1014–1026.
- (8) Yamada, K.; Unno, M.; Kobayashi, K.; Oku, H.; Yamamura, H.; Araki, S.; Matsumoto, H.; Katakai, R.; Kawai, M. Stereochemistry of protected ornithine side chains of Gramicidin S derivatives: X-ray crystal structure of the bis-Boc-tetra-*N*-methyl derivative of Gramicidin S. *J. Am. Chem. Soc.* **2002**, *124*, 12684–12686.
- (9) Kawai, M.; Tanaka, R.; Yamamura, H.; Yasuda, K.; Narita, S.; Umemoto, H.; Ando, S.; Katsu, T. Extra Amino Group-containing Gramicidin S analogs Possessing Outer Membrane-permeabilizing Activity. *Chem. Commun.* **2003**, 1264–1265.
- (10) Kawai, M.; Yamamura, H.; Tanaka, R.; Umemoto, H.; Ohmizo, C.; Higuchi, S.; Katsu, T. Proline residue-modified polycationic analogs of Gramicidin S with high antibacterial activity against both Gram-positive and Gram-negative bacteria and low hemolytic activity. *J. Pept. Res.* **2005**, *65*, 98–104.
- (11) Velkov, T.; Thompson, P. E.; Nation, R. L.; Li, J. Structure-activity relationships of polymyxin antibiotics. *J. Med. Chem.* **2010**, *53*, 1898–1916.
- (12) Rekharsky, M.; Yamamura, H.; Kawai, M.; Inoue, Y. Critical difference in chiral recognition of *N*-Cbz-D/L-aspartic and -glutamic acids by mono- and bis(trimethylammonio)- $\beta$ -cyclodextrins. *J. Am. Chem. Soc.* **2001**, *123*, 5360–5361.
- (13) Yamamura, H.; Rekharsky, M. V.; Ishihara, Y.; Kawai, M.; Inoue, Y. Factors controlling the complex architecture of native and modified cyclodextrins with dipeptide (Z-Glu-Tyr) studied by



microcalorimetry and NMR spectroscopy: Critical effects of peripheral bis-trimethylamination and cavity size. *J. Am. Chem. Soc.* **2004**, *126*, 14224–14233.

(14) Yamamura, H.; Suzuki, K.; Uchibori, K.; Miyagawa, A.; Kawai, M.; Ohmizo, C.; Katsu, T. Mimicking an antimicrobial peptide polymyxin B by use of cyclodextrin. *Chem. Commun.* **2012**, *48*, 892–894.

(15) Yamamura, H.; Shimohara, K.; Kurata, R.; Fujita, Y.; Murata, K.; Hayashi, T.; Miyagawa, A. Unique, Fast, and All-or-none Click Reaction on Cyclodextrin and Amylose. *Chem. Lett.* **2013**, *42*, 643–645.

(16) Yamamura, H.; Sugiyama, Y.; Murata, K.; Yokoi, T.; Kurata, R.; Miyagawa, A.; Sakamoto, K.; Komagome, K.; Inoue, T.; Katsu, T. Synthesis of antimicrobial cyclodextrins bearing polyarylamino and polyalkylamino groups via click chemistry for bacterial membrane disruption. *Chem. Commun.* **2014**, *50*, 5444–5446.

(17) Yamamura, H.; Miyagawa, A.; Sugiyama, H.; Murata, K.; Mabuchi, T.; Mitsuhashi, R.; Hagiwara, T.; Nonaka, M.; Tanimoto, K.; Tomita, H. Rule of hydrophobicity/hydrophilicity balance in membrane-disrupting antimicrobial activity of polyalkylamino cyclodextrins synthesized via click chemistry. *ChemistrySelect* **2016**, *1*, 469–772.

(18) Yamamura, H.; Mabuchi, T.; Miyagawa, A. Syntheses and structure-membrane active antimicrobial activity relationship of alkylamino-modified glucose, maltooligosaccharide, and amylose. *Chem. Biol. Drug Des.* **2017**, *90*, 1012–1018.

(19) Yamamura, H.; Nonaka, M.; Okuno, S.; Mitsuhashi, R.; Kato, H.; Katsu, T.; Masuda, K.; Tanimoto, K.; Tomita, H.; Miyagawa, A. Membrane-active antimicrobial poly(amino-modified alkyl)  $\beta$ -cyclodextrins synthesized via click reactions. *Med. Chem. Commun.* **2018**, *9*, 509–518.

(20) Some of the MIC values against *S. aureus*, *B. subtilis*, and *E. coli* were previously reported. See references 16 and 17.

(21) Lee, M.-T.; Sun, T.-L.; Hung, W.-C.; Huang, H. W. Process of inducing pores in membranes by melittin. *Proc. Natl. Acad. Sci. U.S.A.* **2013**, *110*, 14243–14248.

(22) Katsu, T.; Nakagawa, H.; Yasuda, K. Interaction between polyamines and bacterial outer membranes as investigated with ion-selective electrodes. *Antimicrob. Agents Chemother.* **2002**, *46*, 1073–1079.

(23) Wu, M.; Maier, E.; Benz, R.; Hancock, R. E. W. Mechanism of Interaction of Different Classes of Cationic Antimicrobial Peptides with Planar Bilayers and with the Cytoplasmic Membrane of *Escherichia coli*. *Biochemistry* **1999**, *38*, 7235–7242.

(24) Čujová, S.; Bednářová, L.; Slaninová, J.; Straka, J.; Čerovský, V. Interaction of a novel antimicrobial peptide isolated from the venom of solitary bee *Colletes daviesanus* with phospholipid vesicles and *Escherichia coli* cells. *J. Pept. Sci.* **2014**, *20*, 885–895.

(25) Daugelavičius, R.; Bakienė, E.; Bamford, D. H. Stages of polymyxin B interaction with the *Escherichia coli* cell envelope. *Antimicrob. Agents Chemother.* **2000**, *44*, 2969–2978.

(26) Meletiadis, J.; Pournaras, S.; Roilides, E.; Walsh, T. J. Defining fractional inhibitory concentration index cutoffs for additive interactions based on self-drug additive combinations, Monte Carlo simulation analysis, and *In Vitro-In Vivo* correlation data for antifungal drug combinations against *Aspergillus fumigatus*. *Antimicrob. Agents Chemother.* **2010**, *54*, 602–609.

(27) Idowu, T.; Ammeter, D.; Rossong, H.; Zhanel, G. G.; Schweizer, F. Homodimeric tobramycin adjuvant repurposes novobiocin as an effective antibacterial agent against Gram-negative bacteria. *J. Med. Chem.* **2019**, *62*, 9103–9115.

(28) Nakao, S.; Komagoe, K.; Inoue, T.; Katsu, T. Comparative study of the membrane-permeabilizing activities of mastoparans and related histamine-releasing agents in bacteria, erythrocytes, and mast cells. *Biochim. Biophys. Acta, Biomembr.* **2011**, *1808*, 490–497.

(29) Epand, R. M.; Epand, R. F. Bacterial membrane lipids in the action of antimicrobial agents. *J. Pept. Sci.* **2011**, *17*, 298–305.

(30) Phillips, G. B.; Dodge, J. T. Composition of phospholipids and of phospholipid fatty acids of human plasma. *J. Lipid Res.* **1967**, *8*, 676–681.

(31) Liu, L.; Courtney, K. C.; Huth, S. W.; Rank, L. A.; Weisblum, B.; Chapman, E. R.; Gellman, S. H. Beyond amphiphilic balance: Changing subunit stereochemistry alters the pore-forming activity of nylon-3 polymers. *J. Am. Chem. Soc.* **2021**, *143*, 3219–3230.

(32) Yamashita, H.; Taoka, A.; Uchihashi, T.; Asano, T.; Ando, T.; Fukumori, Y. Single-Molecule Imaging on Living Bacterial Cell Surface by High-Speed AFM. *J. Mol. Biol.* **2012**, *422*, 300–309.

(33) Oestreich, Z.; Taoka, A.; Fukumori, Y. A comparison of the surface nanostructure from two different types of Gram-negative cells: *Escherichia coli* and *Rhodobacter sphaeroides*. *Micron* **2015**, *72*, 8–14.

(34) Jaroslawski, S.; Duquesne, K.; Sturgis, J. N.; Scheuring, S. High-resolution architecture of the outer membrane of the Gram-negative bacteria *Roseobacter denitrificans*. *Mol. Microbiol.* **2009**, *74*, 1211–1222.

(35) Oh, Y. J.; Plochberger, B.; Rechberger, M.; Hinterdorfer, P. Characterizing the effect of polymyxin B antibiotics to lipopolysaccharide on *Escherichia coli* surface using atomic force microscopy. *J. Mol. Recognit.* **2017**, *30*, No. e2605.

(36) French, S.; Farha, M.; Ellis, M. J.; Sameer, Z.; Côté, J.-P.; Cotroneo, N.; Lister, T.; Rubio, A.; Brown, E. D. Potentiation of Antibiotics against Gram-Negative Bacteria by Polymyxin B Analogue SPR741 from Unique Perturbation of the Outer Membrane. *ACS Infect. Dis.* **2020**, *6*, 1405–1412.

(37) Document M100 – Performance Standards for Antimicrobial Susceptibility Testing; 29th edn.; CLSI: Wayne, PA, 2017.

(38) Ando, T.; Koder, N.; Takai, E.; Maruyama, D.; Saito, K.; Toda, A. A high-speed atomic force microscope for studying biological macromolecules. *Proc. Natl. Acad. Sci. U.S.A.* **2001**, *98*, 12468–12472.

(39) Uchihashi, T.; Koder, N.; Ando, T. Guide to video recording of structure dynamics and dynamic processes of proteins by high-speed atomic force microscopy. *Nat. Protoc.* **2012**, *7*, 1193–1206.